Journal of Marine Systems 251 (2025) 104113

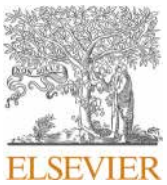

Contents lists available at ScienceDirect

Journal of Marine Systems

journal homepage: www.elsevier.com/locate/jmarsys

Spatial distributions of acoustic scattering groups during the warm-to-cold transition period in the Senegal coastal ecosystem and their relationships with environmental variables

Viviane David [a,*], Jérémie Habasque [a], Gildas Roudaut [a], Louis Marie [b], Delphine Thibault [c], Anne Lebourges-Dhaussy [a], Xavier Capet [d], Eric Machu [b]

[a] IRD, Laboratoire des Sciences de L'environnement Marin (LEMAR) UBO/CNRS/IRD/Ifremer, Plouzané, France
[b] Univ Brest, CNRS, Ifremer, IRD, Laboratoire d'Océanographie Physique et Spatiale (LOPS), IUEM, F29280 Plouzané, France
[c] Aix-Marseille Université, Université de Toulon, CNRS, IRD, MIO, Marseille, France
[d] Laboratoire LOCEAN, CNRS-IRD-Sorbonne Universités, UP MC, MNHN, Paris, France

ARTICLE INFO

Keywords:
Active acoustics
Micronekton
Senegal
Upwelling

ABSTRACT

The coastal area of north-west (NW) Africa is a highly productive ecosystem due to the presence of a strong upwelling. This ecosystem supports large populations of small pelagic fish, such as sardinellas, which have significant socio-economic value for local populations. In this study, we analyzed the acoustic data collected during a one-month survey along the Senegalese coast at the beginning of the upwelling season. Hierarchical clusterings were performed to classify the acoustic data from the epipelagic zone (down to 120 m-depth) separately for daytime and nighttime. The analysis identified five echo-groups during the day and six at night. The resulting echo-groups were then compared to stratified midwater trawl samplings to support hypotheses about the organisms responsible for the echoes. Additionally, a remotely operated towed vehicle (called Scan-fish) was used to monitor environmental variables down to 100 m depth. Two machine learning models were applied to link the classified echo-groups to the environmental data for both day and night. Each daytime echo group had a corresponding nighttime echo group, with also similar environmental preferences. Fish schools were mainly found in shallow coastal waters while dense sound-scattering layers detected at 38 kHz, likely composed of small fish or fish larvae, were observed in the temperature range of 17°-21 °C for both day and night. The other echo-groups were composed of fluid-like zooplankton or gas-bearing zooplankton. The sixth night echo-group corresponded to migrant organisms and was predominant at night. Overall, the analyses of the abiotic habitats for each echo-group allow us to better understand the organism distributions during the beginning of the NW Africa upwelling season.

1. Introduction

The north-west (NW) coastal area off Africa is a highly productive ecosystem that has been exploited by local populations for centuries. The wind regime drives a quasi-permanent offshore Ekman pumping and a seasonal coastal upwelling from November to May, between Cape Roxo (12°20′ N, Senegal) and Cape Blanc (21°N, Mauritania) (Capet et al., 2017). Differences in the shape and slope of the continental shelf induce distinct dynamics in the north and south of the Cape Verde Peninsula (Roy, 1998; Auger et al., 2016). During the upwelling season, spatial variability is particularly pronounced, and turbulent structures such as cold filaments of nutrient-rich waters are present (Strub et al., 1991). Wind-forced upwelling of subsurface, nutrient-enriched water is a key driver of pelagic primary productivity in these coastal waters (Lathuilière et al., 2008; Messié and Chavez, 2015), supporting a strong food web and higher trophic levels. However, its temporal variability is still poorly known (Carr and Kearns, 2003; Auger et al., 2016) and the overall understanding of the NW African upwelling remains limited (Ndoye et al., 2014; Capet et al., 2017). In addition, these ecosystems support large populations of Small Pelagic Fish (SPF) (Roy et al., 1989; Cury and Roy, 1989), such as the sardinellas (Clupeidae), *Sardinella aurita* Valenciennes 1847 and *Sardinella maderensis* Lowe 1838, whose

* Corresponding author.
E-mail address: viviane.david.66@gmail.com (V. David).

https://doi.org/10.1016/j.jmarsys.2025.104113
Received 3 June 2024; Received in revised form 23 July 2025; Accepted 26 July 2025
Available online 27 July 2025

nurseries (Fréon, 1983) are present along the Senegalese coast. Clupeidae are omnivorous, feeding both on phytoplankton and zooplankton (James, 1988) and *S. aurita* and *S. maderensis* represent important resources for industrial and artisanal Senegalese fisheries (Belhabib et al., 2014). Their spawning strategies may rely on the variability of the coastal upwelling intensity as well as on food availability (Demarcq and Faure, 2000; Lett et al., 2006; Mbaye et al., 2015), but this still requires further investigations. In addition, the NW African ecosystem is vulnerable to strong anthropogenic pressures (i.e. overfishing, climate change, pollution) with a risk of disruption across all trophic levels, including the SPF populations (FAO, 2013; Ba et al., 2016). Therefore, a better understanding of the upwelling ecosystem, including the environmental drivers of the SPF population dynamics, is crucial for the sustainable exploitation of the ecosystem.

Active acoustic methods can simultaneously provide information on the distribution of organisms, from zooplankton to top-predators (Benoit-Bird and Lawson, 2016). Calibrated echosounders with several frequency transducers provide information that can be used to classify various types of organisms. With an appropriate frequency range, backscattering sources depending on the organism's complexity (i.e. shape, material properties) can be classified into broad groups. Zooplankton, for instance, can be classified into (i) fluid-like organisms such as copepods or euphausiids, (ii) elastic-shelled organisms such as pteropods, (iii) gas-bearing organisms such as siphonophores (Stanton and Chu, 2000; Lavery et al., 2007). For fish, the presence of a swimbladder is a key parameter influencing their scattering responses, although other parameters like size and behavior can also play a role (Foote, 1987; Kloser et al., 2002). Physical elements such as microstructures, bubbles and suspended sediments can also produce strong scatters (Ross et al., 2007; Lavery et al., 2010). Indeed, microstructures have been shown to contribute significantly to scattering, thus representing a confounding factor when analyzing biological scatterings. Nevertheless, theoretical frequency response curves from biological and physical scattering processes present distinct shapes that can help discriminate them (Stanton et al., 1994b; Warren et al., 2003). Several multifrequency methods have been developed for backscatter classification (De Robertis et al., 2010; Ballón et al., 2011; Béhagle et al., 2017; Choi et al., 2021) based on various approaches (i.e. use differential responses between frequencies or the sum of responses at different frequencies as classification variables). These methods often require a manual annotation by experts, which can be time-consuming, or the definition of thresholds for the acoustic variables, which may involve uncertainties. Furthermore, acoustic studies often consider volume backscattering strengths, rather than target strengths, for logistical reasons and because a group of organisms with similar properties would keep the same frequency response curve (Benoit-Bird and Lawson, 2016). Overall, multiple factors including organism types, size, behavior and orientation induce variable scattering echo levels (Stanton et al., 1994a; Zedel et al., 2005), making organism identification in active acoustics more challenging. To address this issue, alternative methods such as the forward method using theoretical scattering models have been developed (Stanton et al., 1994a, 1998; Blanluet et al., 2019; Barbin et al., 2024). These models predict the theoretical scattering signals from the organisms sampled by trawl, which can then be compared to the observed signal on echograms. However, this approach often requires biological samplings with a good knowledge of the taxa present, as well as their morphological characteristics within scattering layers, to reduce uncertainties in scattering signal estimation (Barbin et al., 2024).

Furthermore, active acoustic methods have been used to study Mid-Trophic-Level Organisms (MTLOs), or micronekton, which include organisms ranging in size from 1 to 20 cm (fish, crustaceans, mollusks, and gelatinous organisms) and are present in all oceans (Brodeur et al., 2005). In particular, characteristic Sound Scattering Layers (SSLs) of zooplankton and micronekton were identified during an upwelling event along the Senegalese continental shelf by Diogoul et al. (2020). MTLOs play an important role in the food web, as they are predated by higher trophic levels, including high value commercial species such as tuna (Bertrand et al., 2002; Lehodey et al., 2015). Zooplankton and micronekton perform extensive Diel Vertical Migrations (DVMs), mostly to feed and acquire energy in the upper layer (0–200 m) at night before migrating back down to the mesopelagic zone (200–1000 m) to avoid predation and reduce metabolic expenditures during the day (Cushing, 1951; Bollens and Frost, 1989a, 1989b; Hays, 2003; Lampert, 1989). These migrations contribute actively to vertical fluxes of nutrients and organic matter (Hays et al., 1997; Ariza et al., 2015; Cotté et al., 2022). Furthermore, DVM behavior is thought to be influenced by various environmental factors such as food availability, dissolved oxygen concentration, light intensity and turbidity. A deeper understanding of these factors is needed as DVM likely results from a complex set of trade-offs (Klevjer et al., 2016). In particular, dissolved oxygen concentration may strongly influence vertical migration patterns and swimming speed depending on the species (Mutlu, 2006; Bianchi et al., 2013).

Several active acoustic studies focus on the coast of west Africa (Demarcq and Samb, 1991; Sarré, 2017; Diogoul et al., 2021; Mouget et al., 2022) to better understand this ecosystem. Especially, acoustic data were compared with environmental data to study the upwelling ecosystem in this region. Diogoul et al. (2020) showed differences in the distribution and structure of the SSLs in inshore and offshore areas during an upwelling event. In particular, the vertical distribution of SSLs was linked to strong vertical gradients of temperature, dissolved oxygen, and water density. Moreover, the long-term distributions from 1995 to 2015 of two acoustic groups (zooplankton and fish) monitored at 38 kHz in this area were compared with sea surface environmental data (Chlorophyll-a concentrations, temperature), showing that the marine pelagic resources (fish and zooplankton) remained stable despite year-to-year variability (Diogoul et al., 2021). Nevertheless, upwelling dynamics offshore of Senegal have been mostly analyzed using satellite and sometimes in situ measurements (Capet et al., 2017), which limits our understanding. Although a bi-frequency (38 and 120 kHz) method have been used to discriminate copepods of the West Africa coast (Diogoul et al., 2024), the application of a multifrequency method to classify the acoustic data for a better ecosystem-based understanding of this area is still lacking and would be highly beneficial.

In this context, the objective of the study was to provide new insights into the spatial distributions of different acoustic groups in the NW African ecosystem in relation to the environmental conditions measured throughout the water column, within the upwelling context. To achieve this, we first classified the acoustic data collected during the survey into distinct echo-groups using a multifrequency approach and compared the results with stratified midwater trawl samplings to hypothesize the associated organisms. Secondly, we investigated the environmental preferences of each echo-group by coupling the acoustic data with environmental measurements down to 100 m obtained using a remotely operated towed vehicle (Scanfish) and by applying machine learning models based on the XGBoost algorithm (eXtreme Gradient tree Boosting) (Receveur et al., 2020).

2. Material and methods

2.1. Survey

The SCOPES survey (DOI: 10.17600/18000662) took place from December 17, 2022 to January 5, 2023, onboard the French Research Vessel RV *Thalassa* and covered the Senegalese coast (12°N-17°N, Fig. 1) at the beginning of the upwelling season. High number of fishing boats at night limited our capacity to conduct samplings over the shallow areas (< 100 m), which were mainly sampled during the day, while deeper areas (≥ 100 m) were mainly sampled at night. The survey route was adjusted along the way to sample waters reflecting contrasting environmental conditions. Filaments were identified using satellite observations of ocean colour (OC) retrieved from a global ocean gridded L3

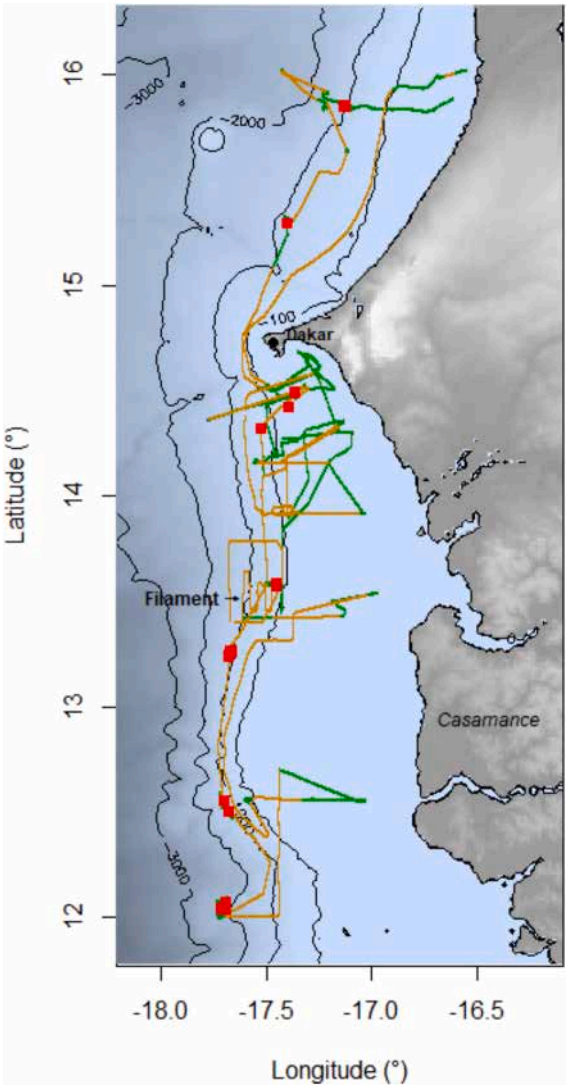

Fig. 1. Cruise tracks of the survey conducted from the RV Thalassa along the Senegalese coast. The plain lines (orange and green) represent the ship track for which the EK80 echosounder recorded data. The orange line represents the portions for which the Scanfish was towed behind the vessel. Red squares represent trawl sampling positions. The thin black lines represent the isobaths. The location of the explored filament at 13.5°N is indicated by an arrow. (For interpretation of the references to colour in this figure legend, the reader is referred to the web version of this article.)

daily product of Copernicus Marine Service with a 300 m × 300 m resolution (European Union-Copernicus Marine Service, 2022). In particular, sampling was conducted across a filament located at 13.5°N visible on OC images (e.g. 12/20/2022, Fig. 1).

2.1.1. Active acoustic data

In situ active acoustic data were recorded continuously using an EK80 echosounder (Simrad, Kongsberg) in continuous wave (CW) mode, connected to six split-beam transducers (18, 38, 70, 120, 200 and 333 kHz) (Fig. 1), of which only five provided useful data (the 18 kHz was dysfunctional and gave an unusable signal over the upper 100 m). The remaining five transducers had a nominal aperture of 7° at −3 dB. Calibration of the EK80 echosounder following standard protocol (Demer et al., 2015) was conducted in April 2022. The water column was sampled down to 800, 450, 250, 120 and 80 m, which were the maximum ranges in this survey respectively for the 38, 70, 120, 200 and 333 kHz transducers. Transmit powers were of 2000, 600, 200, 90 and 40 W respectively for the five channels and the pulse length was set at 1024 μs for all frequencies. Mean vertical resolution according to this pulse length was 0.789 m. Two ping intervals were set depending of the bathymetry, with a pivot depth at 200 m: 0.6 s in shallow waters and 2.6 s in deep waters. Data were acquired at a vessel speed of ~8 knots.

2.1.2. Environmental data

A total of 46 casts (Seabird SBE 911+) were conducted throughout the survey. Sea surface environmental variables (temperature, salinity and Chl-a) were continuously recorded by a thermosalinograph and a Ferrybox system (Petersen, 2014). A Scanfish II (Brown et al., 1997), equipped with a CTD SBE49 (reference 201), a SBE43 (reference 430,214) and an ECO Triplet (reference BBFL2WB-1478) measured the temperature and salinity at a rate of 0.06 s and the Chl-a concentrations and dissolved oxygen at a rate of 1 s from the surface down to ~100 m depth. Approximately 2500 profiles were collected during the 127 h of deployment. As the Scanfish was towed between 300 and 600 m astern of the ship (depending on location and bathymetry, Fig. 1), acoustic and Scanfish data were not perfectly collocated. To correct for the mismatch, we computed an offset time for the Scanfish relative to the echosounder based on the mean vessel speed and separation distance between the Scanfish and the transducer's location onboard the vessel.

2.1.3. Biological samples

A total of 11 micronekton trawls (Table S1) were conducted in the upper layer (down to 70 m) at various stations (Fig. 1 and Table S1) to sample key acoustic layers. The micronekton trawl had a mesh size of 80 mm at the entrance, reduced to 10 mm at the codend. Trawl depth, as well as vertical and horizontal openings in meters, were monitored in real-time with net sensors (Marport® Trawl Explorer, Reykjavik, Iceland), with the net vertical opening generally around 10 m. A Wildlife Computers TDR (Time Depth Recorder) was attached to the back rope to monitor pressure at a recording rate of 1 s. The protocol was standardized for each trawl: (i) the fishing depth was first chosen based on the echograms, then (ii) the net was stabilized at the echo depth using the MARPORT depth-positioning device, and (iii) the net was towed 30 min at a vessel speed of 2–3 knots. Collected zooplankton and micronekton were sorted onboard by broad taxonomic groups (e.g., fish, crustaceans, squids, gelatinous organisms) before being stored at −20 °C. The most sensitive species were stored with water to preserve their morphological structure.

2.2. Acoustic data processing

All raw acoustic data were processed using the open-source Matecho software (Perrot et al., 2018). Automatic bottom detection and data cleaning were applied to remove unwanted detections including ghost bottom echoes and interferences from other acoustic devices. Empty pings were discarded and background noise reduction was made (De Robertis and Higginbottom, 2007). To suppress the near-fields effects and surface noise, the first 8 m from the surface were removed for all frequencies. After pre-processing, data were echo-integrated into 1 m vertical layers and over 0.05 nmi Elementary Sampling Unit (ESU) using a − 100 dB minimal threshold. The echo-integration was performed from 10 m down to the maximum range of each frequency (DOI: 10.17882/96903). Sound celerity and Time Varying Gain (TVG) corrections were applied using temperature and salinity profiles from the 46 CTD casts collected during the survey. The closest-in-time CTD cast was used for each ping to recalculate the TVG. For each echointegrated cell, the mean volume backscattering strength (S_v in dB, re 1 m^{-1}) was calculated for each frequency (MacLennan et al., 2002) as well as their coefficients of variation (CVs), defined as the ratio of the standard deviation to the mean. The linear form of the volume backscattering strength s_v (m^{-1}) was used for all required calculations (e.g. in the echo-integration step procedure, the CV calculations and the map representations). Finally, the Nautical Area Scattering Coefficient (NASC or s_A, m^2 nmi^{-2}) was

calculated per ESU of 0.05 nmi, according to MacLennan et al. (2002), providing a proxy of biomass.

2.3. Statistical analysis

2.3.1. Data clustering

As the Scanfish operated from the surface down to 100 m depth, only the 38, 70, 120 and 200 kHz frequencies were used to classify echoes, as data acquired with the 333 kHz frequency does not cover this depth range. The echo-integrated cells ranging from 10 to 120 m were used for clustering. During the cruise, the activity of artisanal fishermen prevented us from occupying the continental shelf at night. This field constraint limited our ability to explore diurnal cycle behaviors. Crepuscular periods (sunrise and sunset) were excluded from the clustering as they are associated with rapid vertical displacements of many organisms and strong variations in the individual orientations.

Hierarchical clusterings were performed using the Ward2 method, which minimized the total within-cluster variance (sum-of-squares criterion). The clusterings were carried out using 12 variables described below. First (i), as often used in multifrequency classifications (De Robertis et al., 2010), we used pairwise frequency differences for each echointegrated cell (i.e., $\Delta S_{v,i-j} = S_{v,i} - S_{v,j}$, where i and j are indices corresponding to two different frequency in kHz). It resulted in six possible pairwise combinations for a total of four frequencies ($\Delta S_{v,70-38}$, $\Delta S_{v,120-38}$, $\Delta S_{v,200-38}$, $\Delta S_{v,120-70}$, $\Delta S_{v,200-70}$ and $\Delta S_{v,200-120}$). To enhance the contrast between fish and macrozooplankton backscatters, we summed (ii) the mean volume backscattering strengths (Ballón et al., 2011) for each echointegrated cell using three frequencies ($S_{v,38} + S_{v,70} + S_{v,120}$ and $S_{v,70} + S_{v,120} + S_{v,200}$). These two sums were specifically chosen because resonance at lower frequencies such as 38 kHz is pronounced for fish with swimbladders whereas low backscattering organisms such as zooplankton scatters at higher frequencies (Lavery et al., 2007; Davison et al., 2015). Finally, we used (iii) the coefficients of variation (CVs) of the volume backscattering strengths at four frequencies (CV_{38}, CV_{70}, CV_{120} and CV_{200}) for the clustering process as they can add effective discriminant information (David et al., 2024). Weighting these variables have been also tested to enhance classification accuracy. Then, the Within-Cluster Sum of Squares (WSS) curves were computed to identify the optimal numbers of clusters, minimizing WSS for night and day separately. We subsequently compared the results to the Ward-linkage cluster dendrogram plots to verify that these numbers of clusters were appropriate. Finally, for nighttime, the clustering process was rerun for one of the clusters to separate the echo-integrated cells scattering strongly at 70 kHz. These cells were not well clustered at first due to their lower cell number at night. To perform the hierarchical clusterings, we used the « fastcluster » package of R (version 4.2.2) which can handle large datasets.

2.3.2. Echo-group interpretations

Hereafter, the different clusters were referred to « echo-groups ». For each echo-group, the Nautical Area Scattering Coefficient (NASC or s_A, m^2 nmi^{-2}, MacLennan et al., 2002) was calculated. In addition, the frequency response curves were analyzed with reference to theoretical scattering models from the literature (Lavery et al., 2007). For this purpose, acoustic data measured at 333 kHz for each echo-group, for depths appropriate to this frequency, were also used to obtain broader frequency response curves.

Trawl data were analyzed as follows. At each trawl station (Table S1), echoes within the sampled layer were extracted by overlaying trawl tracks onto echo-integrated echograms using the pressure recorded by TDR and a 10 m vertical opening. The trawl was towed behind the vessel, so an offset time for the trawl data was computed in the same manner as for the Scanfish data (see Section 2.1). For each echo-group, the echo cells within the depth range of the trawl track were extracted. The number of cells per echo-group found in the trawl were then computed. Finally, acoustic results for each trawl were compared to its biological content. Correlation matrices using the Pearson method were used to relate the number of echo-integrated cells per echo-group to the weight proportions of each group of organisms found in the trawls. Especially, as suggested by Mutlu (2007), we multiplied the weight of the organisms by their reflection coefficients (R) (Table S2) to improve the correlation matrices. Three matrices were calculated, using separately the day or night data, as well as for day and night combined.

2.3.3. XGBoost models

To analyze the relationship between acoustic echo-groups and environmental conditions, we applied the XGBoost algorithm (eXtreme Gradient tree Boosting). This "machine-learning" method has already been used for active acoustic data (Receveur et al., 2020). The environmental variables provided by the Scanfish and surface variables (temperature, salinity and Chl-a) were used for the modelling. Environmental data were averaged at the same resolution as the acoustic data (cells of 0.05-nmi wide and 1-m deep). As the Scanfish was not deployed during the entire survey, only periods with simultaneous acoustic and Scanfish acquisitions were kept for these analyses.

Two models were built separately for daytime and nighttime. The models were first fitted on a training dataset (75 % of the data randomly chosen) and then tested on a validation dataset (the remaining 25 %). Concerning the XGBoost parameters, the learning rate η was set to 0.5 and six maximum tree depths were chosen to prevent over-fitting. For each model, statistical information such as accuracies and their 95 % confidence interval (CI), sensitivities and specificities were computed (Kuhn, 2008). A manual backward selection of the variables was made in order to keep the best models. To build the models, we used the « xgboost » package available in R (Chen and Guestrin, 2016). As in Receveur et al. (2020), SHapley Additive exPlanation (SHAP) values were computed to rank the importance of covariates for the overall models and for each echo-group. SHAP values indicated how much a given covariate value would change the predicted value compared to a prediction made without this covariate (Lundberg and Lee, 2017). 1000 Monte Carlo simulations were performed (Štrumbelj and Kononenko, 2014) to approximate the SHAP values for the different echo-groups.

3. Results

3.1. Environmental conditions over the southern Senegalese shelf

Sea surface environmental variables were highly variable along the Senegal coast during the SCOPES survey (Fig. S1). Temperatures ranged from 19° to over 27 °C. The lowest temperatures were recorded in areas of coastal resurgence, particularly to the north (15°N and 16°N) and south of the Cape Verde Peninsula. Coastal waters were bordered by warmer offshore waters and a progressive cooling of surface waters was observed throughout the survey. For instance, surface water temperatures were closed to 27 °C at the beginning of the survey and 23 °C at the end of the survey for offshore waters at 14°20′N (Fig. S1a). In response to subsurface upwelling, the coldest waters were also the saltiest. These colder, saltier areas were associated with the highest surface phytoplankton biomass and oxygen levels, suggesting developing phytoplankton biomass. A notable exception was found in the south (12.5°N), where enrichment was observed but salinity remained low (Fig. S1b). Localized patches of high sea surface Chl-a concentrations were observed in shallow waters (< 100 m), mostly close to the coast (Fig. S1c). At the start of the survey (between December 17 and 25), waters off the shelf and in the southern part of the system presented salinities 1 unit lower than over the northern part of the shelf. This highlighted the influence of freshwater inflows during the monsoon season from the southern regions of the system, which were then transported northward by the West African Boundary Current (Kounta et al., 2018).

As the vessel repeatedly crossed the filament at 13.5°N, vertical shifts

of the environmental conditions were observed (Fig. 2). The position of the subsurface chlorophyll maximum varied between 40 and 10 m depth. In addition, average vertical profiles of the environmental variables (down to 100 m-depth; Fig. S2) were shown for daytime and nighttime. For both periods, sharp transitions were observed between 40 and 20 m depth for temperature, dissolved oxygen and salinity. Chl-a concentrations were higher during the day with a maximum above 20 m depth and values >1 µg.L^{-1} when the maximum was located around 30 m depth and ~ 0.7 µg.L^{-1} during the night.

3.2. Description of the echo-groups

The NASC distributions along the track for both daytime and nighttime was given at 38 kHz, a frequency for which some organisms like fish with swimbladders can have strong resonance (Fig. S3). It showed higher biomass concentrations (represented in red) at specific locations: north of the survey tracks, south of the Cap Verde peninsula and near Casamance.

Two hierarchical clustering were constructed based on 1,301,856 and 750,482 cells for nighttime and daytime, respectively. Adding the CVs and the two sums ($S_{v,38} + S_{v,70} + S_{v,120}$ and $S_{v,70} + S_{v,120} + S_{v,200}$) provided additional information for the clustering, which was crucial to be able to separate pelagic fish schools from scattering layers. Nevertheless, *Sv* differences were key information for separating the other scattering groups, except for fish schools, and were weighted by a factor 2 to optimize the clustering and obtain different frequency response curves. Based on the WSS curves (Fig. S4a,b), the curve bend occurred between 5 and 6 clusters. Indeed, the WSS curves decreased rapidly between one and six clusters, after which the slope flattened. We compared these results with the Ward-linkage cluster dendrogram plots (Fig. S4c,d), and confirmed that 5 and 6 echo-groups were adequate respectively for daytime and nighttime. Selecting 6 clusters for nighttime was also more biologically interpretable and facilitated the comparison with the daytime echo-groups. Thereafter, the echo-groups will be numbered D1 to D5 for daytime and N1 to N6 for nighttime. Examples of the echogram and the corresponding echo-groups for daytime and nighttime are shown in Fig. 3.

Note that numbering (from 1 to 5) was chosen such that day and night echo-groups with the same number had the most similar acoustic characteristics among echo-groups, based on the frequency response curves (Fig. 4). Additional information on the different echo-groups can also be found on Figs. S5 to S9. The NASC distribution along the Senegalese coast also differed between the echo-groups (Fig. 5). More precisely, the D1 and N1 echo-groups were characterized by frequency response curves, or $S_v(f)$ curves, with increasing acoustic density between 70 and 333 kHz, which could correspond to fluid-like organisms (Lavery et al., 2007), but with a peak observed at 38 kHz. These echo-groups were found over all bottom depth but mainly in the deeper areas ($>$ 100 m) (Figs. 4a,f and 5). The D2 and N2 echo-groups were characterized by high values at 70 kHz and decreasing curves between 70 and 333 kHz (Fig. 4b,g). Such a shape could correspond to gas-bearing organisms (e.g. physonects or cystonects siphonophores) (Lavery et al., 2007; Blanluet et al., 2019). D2 was found mainly south of the Cap Vert peninsula, while N2 was located along the entire Senegalese coast, both over the shelf and at the shelf break. The D3 and N3 echo-groups were characterized by decreasing $S_v(f)$ curves from 38 to 333 kHz (Fig. 4c,h) and could correspond to fish larvae or small fish with swimbladders. These echo-groups were located along the entire Senegalese coast, with higher biomass in areas with depth $\geq$ 30 m. The D4 and N4 echo-groups had similar $S_v(f)$ curves to D3 and N3 (Fig. 4d,i), but with a higher density at 38 kHz and with the lowest CVs for each frequency. They could also correspond to fish larvae or small fish with swimbladders (Lavery et al., 2007). Their distributions were patchier along the Senegalese coast. The D5 and N5 echo-groups were characterized by high values of CVs and, for D5, combined with high values for the sum of frequencies. These echo-groups were associated with a flat curve with high S_v values (Fig. 4e,j) which could correspond to frequency responses of fish with swimbladders. Visual inspections of the echogram confirmed that D5 and N5 corresponded to schooled fish (mostly for daytime) or isolated fish (mostly nighttime). Higher proportions of D5 and N5 were encountered close to the coast and mostly south of the Cap Vert peninsula. Finally, the last echo-group N6 was characterized by a decreasing $S_v(f)$ curve from 38 to 333 kHz but showed a small relative maximum at 120 kHz compared to 70 and 200 kHz (Fig. 4k). It could also correspond to $S_v(f)$ curves of small fish or fish larvae with swimbladders. This N6 echo-group was located along the entire Senegalese coast.

Finally, for daytime, the D3 echo-group regrouped 41 % of the cells while D1 represented 23 %; D4: 22 %; D2: 10 % and D5: 4 %. For nighttime, the N6 echo-group gathered the majority of cells (39 %)

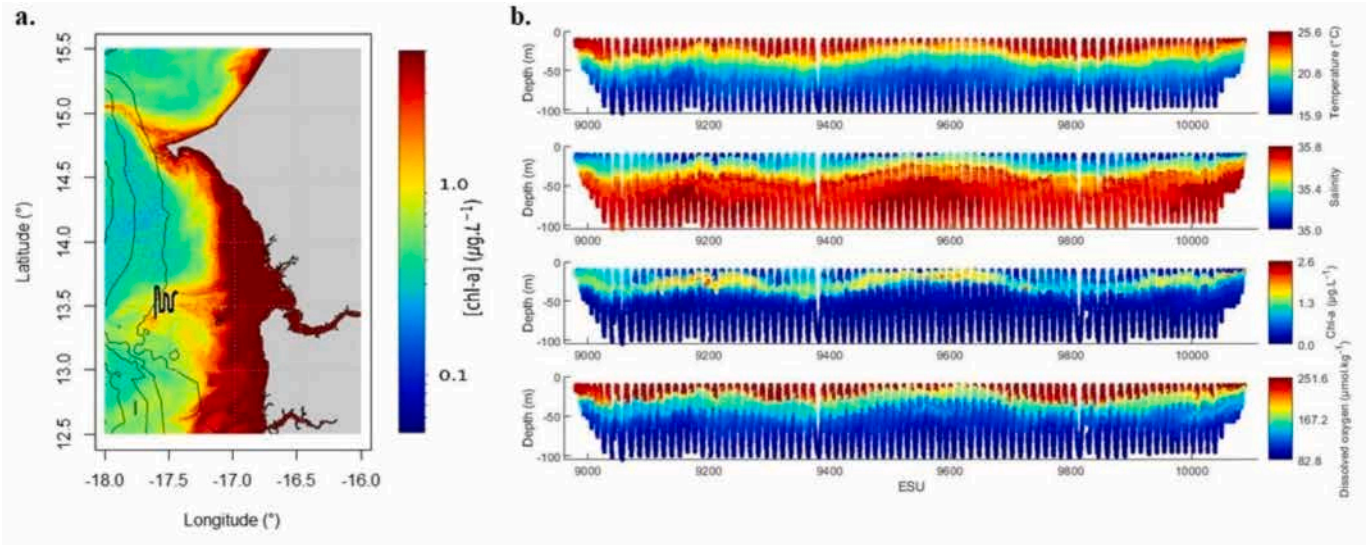

Fig. 2. (a) Satellite observations of Chl-a concentrations observed on 12/20/2022 during the survey. The black line corresponds to the transect made by the vessel across the 13.5°N filament. Observations of ocean colour (OC) were retrieved from European Union-Copernicus Marine Service. (b) Sequence of Scanfish profiles across the filament at 13.5°N. From top to bottom, vertical profiles of temperature, salinity, Chl-a, and D.O. concentrations. Data were recorded from 8 p.m. the 12/21/2022 to 4 a.m. the 12/22/2022. ESU means Elementary Sampling Unit.

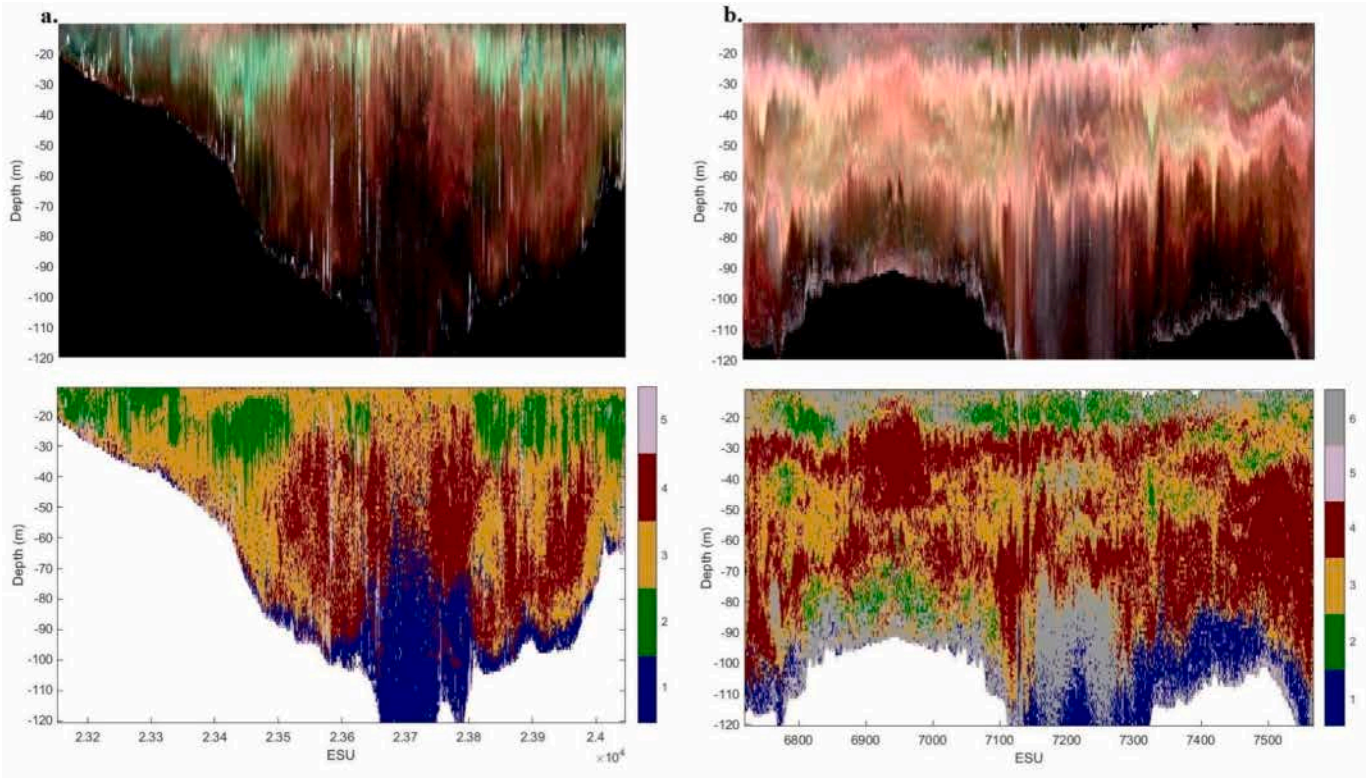

Fig. 3. Examples of echograms and the corresponding echo-groups during daytime (a) and nighttime (b). The echograms are presented in Red Green Blue (RGB) composite images generated with MATLAB based on the 38 (red), 70 (green) and 120 (blue) kHz echo-integrated acoustic data. The echo-groups D1 to D5 and N1 to N6 are represented by colors (blue, green, yellow, red, purple, and grey respectively). ESU means Elementary Sampling Unit. (For interpretation of the references to colour in this figure legend, the reader is referred to the web version of this article.)

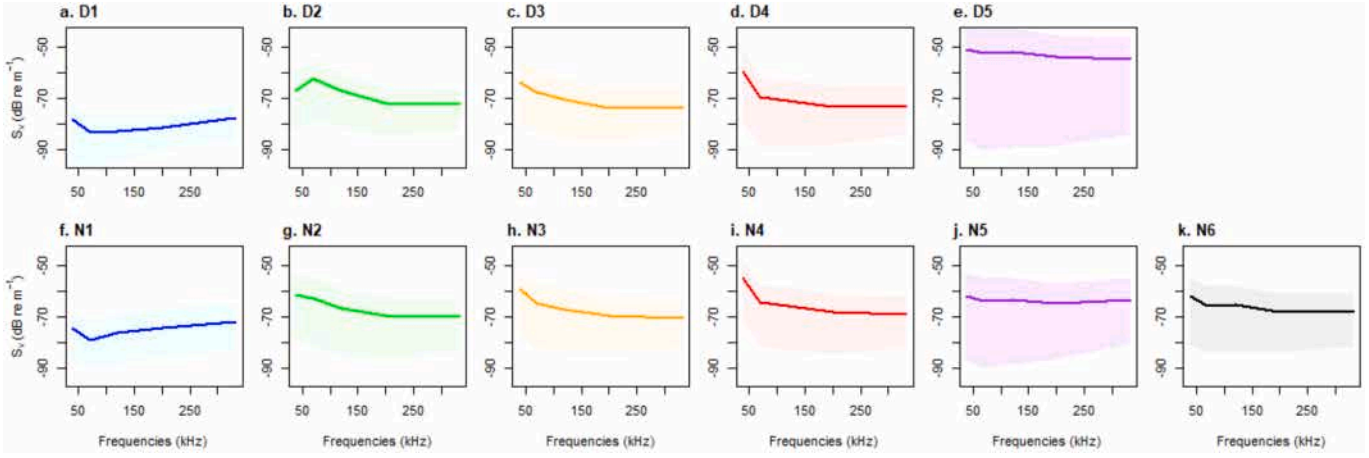

Fig. 4. Frequency response curves of the echo-groups from daytime (panels a to e) and nighttime (panels f to k). Blue, green, red, yellow, purple, and dark lines are for the echo-groups 1 to 6, respectively. Light shaded areas represent the 95 % confidence interval. (For interpretation of the references to colour in this figure legend, the reader is referred to the web version of this article.)

followed by N3 (23 %) and the other echo-groups (N1: 15 %; N4: 11 %; N2: 9 % and N5: 3 %). In addition, we observed that despite the fact that the sampling areas were not exactly the same during daytime and nighttime (shallow waters vs offshore), the nighttime echo-groups were very similar to the daytime ones, except for N6. Indeed, to compare with daytime, proportions for the nighttime were also calculated excluding the N6 echo-group, as it was only present during nighttime. The obtained proportions were then equivalent to those for daytime, N3: 38 %; N1: 25 %; N4: 18 %; N2: 15 %; and N5: 4 %.

3.3. *Echo-group interpretations with regards to trawl contents*

We aimed to validate the interpretation of the echo-groups in terms of dominant marine organisms with the trawls' content. Distribution maps of the biological content of all trawls for daytime and nighttime can be found in Supplementary Information (Fig. S10). During daytime, gelatinous organisms and fish were caught, but the biomass collected was very low (Table S1 and Figs. S11 to S15), except for trawl T5_D. Hence, linking the daytime echo-groups to the trawl data was not straightforward, and results of the correlation matrix for daytime

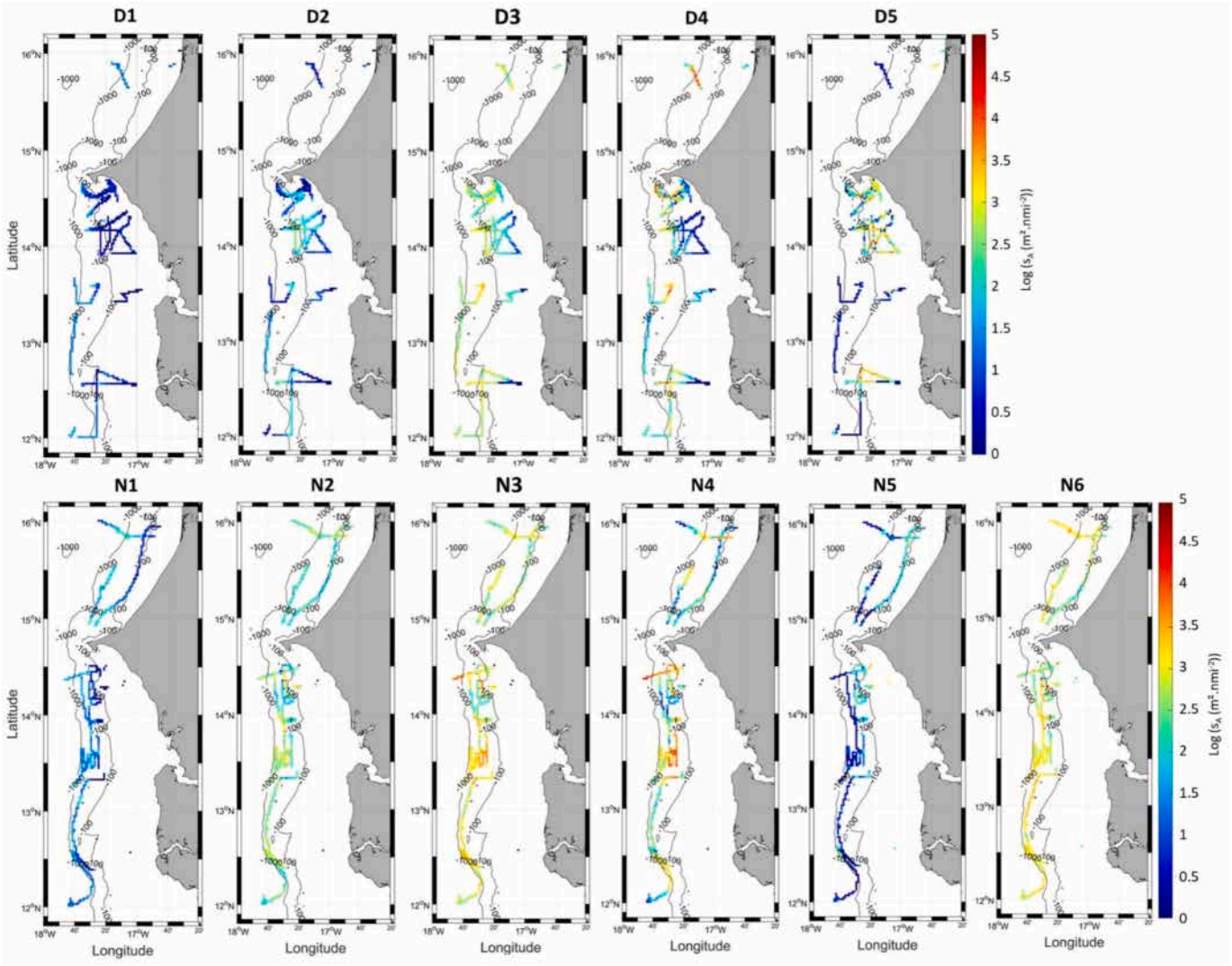

Fig. 5. Spatial distributions of the echo-groups along the Senegalese coast during SCOPES (17 December to 05 January). The colors represent the acoustic density of the Nautical Area Scattering Coefficient (NASC, m^2 nmi^{-2}) at 38 kHz. Top panels are for daytime (D1 to D5) and bottom panels are for nighttime (N1 to N6).

(Fig. 6a) should be interpreted with caution. Overall, the D1 echo-group showed a positive correlation with crustaceans, squids, gelatinous, and fish larvae. The D2 echo-group was primarily positively correlated to siphonophores, but also to crustaceans and fish. The D3 and D4 echo-groups were both positively correlated to fish, with D3 also correlated with squids and gelatinous organisms and D4 also correlating with fish larvae, pyrosomes and crustaceans. Finally, the D5 echo-group was correlated to gelatinous organisms.

During nighttime, fish, gelatinous organisms, crustaceans and cephalopods were caught in the trawls, with fish being the most abundant in all trawls (Figs. S16 to S21). In particular, myctophids were present in all night trawls except for trawl T9_N (Table S1). This specific trawl was mainly composed of other fish species. A high quantity of cephalopods was captured only in trawl T6_N, in combination with fish species. Finally, only a few siphonophores were captured during nighttime.

All echo-groups were found in the last trawl (T11_N, Fig. S21) conducted during nighttime, which was consistent with the high abundances of various organisms observed in this trawl. Globally, the N2, N3, N4 and N6 echo-groups were the most preponderant in trawls during nighttime. Moreover, the N1 echo-group was mostly positively correlated to shrimps, euphausiids, siphonophores and tetraodontidae (Fig. 6b). The N2 echo-group was positively correlated to squids and myctophids (Fig. 6b). Nevertheless, the N2 echo-group was only preponderant (46 %) in trawl T6_N. This trawl was heterogeneous, mainly composed of gelatinous organisms, squids and fish species, making the interpretation in terms of echo-group difficult. The N3 and N4 echo-groups were present when fish or fish larvae were caught, but the association is ambiguous because gelatinous organisms, crustaceans and cephalopods were often caught in the same trawls. Indeed, the N3 echo-group was mostly positively correlated with fish larvae, gelatinous and crustaceans (Fig. 6b) and the N4 echo-group was mostly positively correlated with fish and shrimps (Fig. 6b). The N5 echo-group was only important in T9_N, where fish belonging to the families Sphyraenidae, Scombridae and Priacanthidae were caught, which could explain the strong N5 echoes. Indeed, the N5 echo-group was positively correlated with these fish families (Fig. 6b).

Furthermore, comparing the correlation matrices using data from both daytime and nighttime to the one using only data from nighttime was informative, as it provided globally similar results for all echo-groups. This could be related to the fact that trawl catchability was greater at night. For example, results for the N5 echo-group were very similar for the matrices using only nightime data (Fig. 6b) and the one using both daytime and nighttime data (Fig. 6c), showing that daytime trawls were not informative for this echo-group.

Comparing these correlation matrices was helpful to interpret the N6

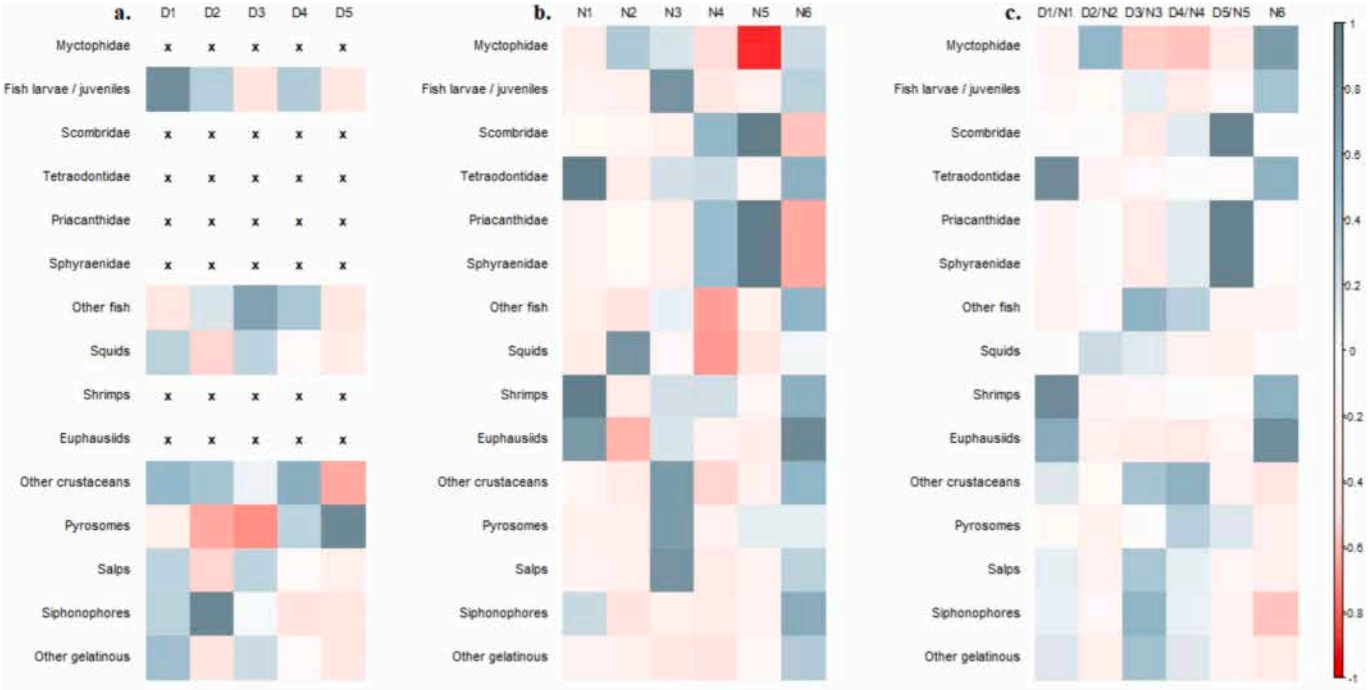

Fig. 6. Correlation matrices relating the number of echo-integrated cells per echo-group to trawl biological contents for day (a) and night (b) separately, and for day and night combined (c). The colors correspond to the correlation values. Each column represents an echo-group, which should be interpreted in relation to the blue squares, indicating positive correlations with a group of organisms, taking into account their weight in trawls and their reflection coefficient (R). The crosses in panel a indicates that these organisms were absent from daytime trawls. (For interpretation of the references to colour in this figure legend, the reader is referred to the web version of this article.)

Table 1
Echo-group interpretations. Summary of the hypothesis and overall confidence.

Echo-groups	Type of organisms	Elements of support	Overall confidence	Comments
D1 and N1	Fluid-like zooplankton mixed with other organisms	Increasing $S_v(f)$ curves between 70 and 333 kHz, with a peak at 38 kHz, consistent with trawl analysis	Medium	Responses that may be polluted by higher scatters
D2 and N2	Organisms with a pneumatophore	Decreasing $S_v(f)$ curves with a peak at 70 kHz	Low	
D3 and N3	Fish larvae or small fish	Decreasing $S_v(f)$ curves, scattering at 38 kHz but lower peaks than for D4 and N4	Low	Possible mix of organisms and/or lower biomass than D4 and N4
D4 and N4	Fish larvae or small fish	Decreasing $S_v(f)$ curves, scattering at 38 kHz, observations of SSLs	Medium	
D5 and N5	Schools and isolated fish	Flat $S_v(f)$ curves, observations of schools and isolated fish on the echogram, consistent with trawl analysis	High	
N6	MTLOs	Decreasing $S_v(f)$ curves, only found at night, observations of vertical migrations and consistent with trawl analysis	High	

echo-group. Indeed, this echo-group was absent during daytime, and adding day and night data highlighted taxa only present at night (Fig. 6b,c), such as myctophidae. On the contrary, for the D3 and N3 echo-groups which were present both during daytime and nighttime, the correlation coefficient was lower for myctophidae in Fig. 6c compared to Fig. 6b as these organisms were only present at night. Finally, results showed that the N6 echo-group was positively correlated with several type of organisms such as fish (including myctophidae), squids, shrimps and euphausiids (Fig. 6c). Indeed, the N6 echo-group appeared (up to 53 %) whenever micronektonic species were caught during nighttime (Table S1). Conversely, the lowest proportion of N6 (15 %) was observed in trawl T9_N, in which myctophids were absent (Fig. S19). This echo-group could then represent micronektonic species. This finding was further supported by visual observations of the N6 layers performing DVM (e.g. Fig. S22). For clarity, the echo-group interpretations are summarized in Table 1.

3.4. Environmental factors driving the echo-groups

Among the potential explanatory variables, those associated with the sea surface were the least important covariates. They were removed from the retained models to increase their accuracies (data not shown). Model accuracy was higher for daytime (0.75 and 95 % CI [0.74, 0.79]) than for nighttime (0.59 and 95 % CI [0.58, 0.59]). Detailed statistics by echo-groups can be found in Tables S3 and S4. Sensitivity and specificity differed between echo-groups, N4, N6, D1, D2 and D3 were better predicted than N2, N5 and D5. The SHAP values were calculated for the entire models for both day and night periods (Fig. S23). The variables that best explain the models were temperature, local bathymetry, and latitude; with Chl-a concentrations also being important for the daytime model.

SHAP values calculated for each echo-group are given in Figs. 7 and 8, and plots of the SHAP values for each explanatory variable and each echo-group are shown in Figs. S24 and S25 (e.g.). The D1 and N1 echo-groups were associated with low temperature (< 18 °C) combined with

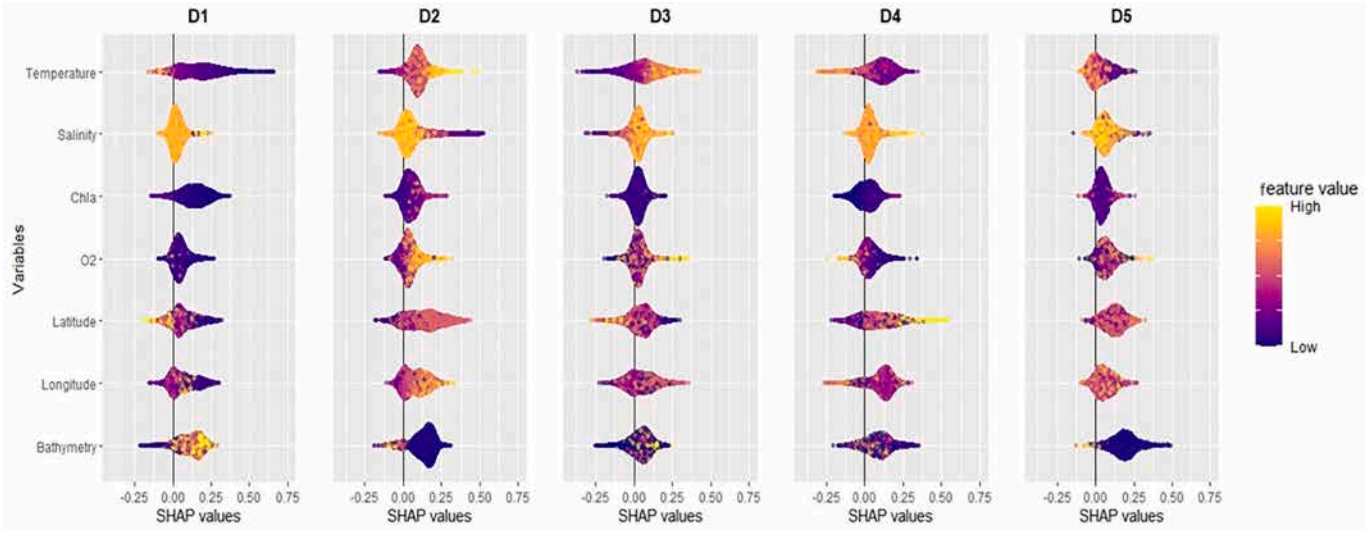

Fig. 7. SHAP (SHapley Additive exPlanation) values for each echo-group from daytime. The dot colour represents the normalized values for each variable (Low and high refers respectively to the minimum and maximum values for the considered variable, e.g. temperature). 1000 Monte Carlo simulations were made to compute the SHAP values for each echo-group.

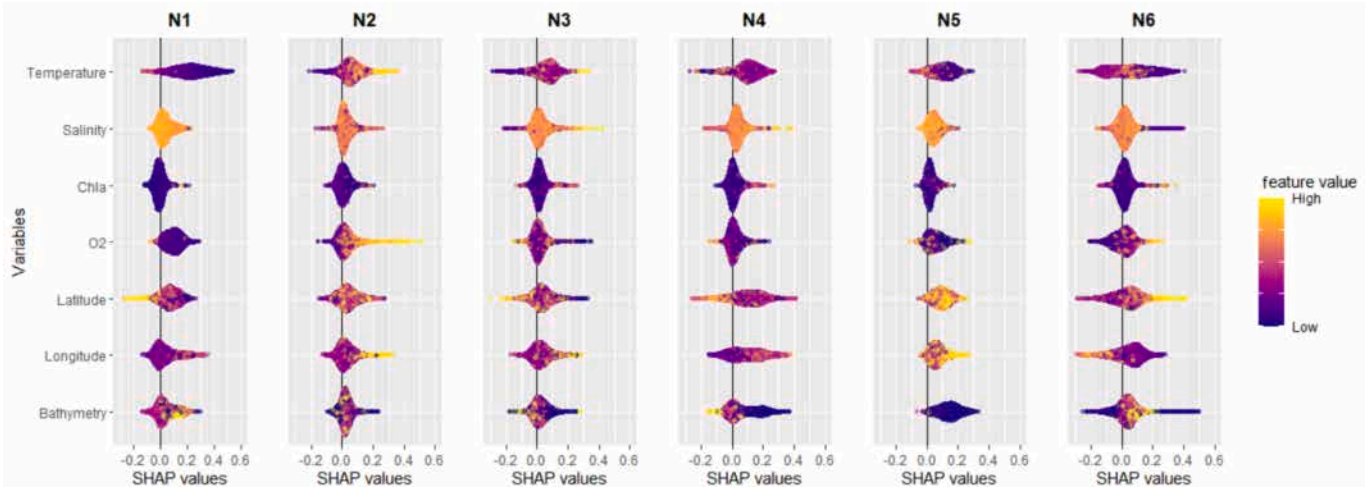

Fig. 8. Same as Fig. 7 for nighttime.

high salinity (> 35), deep bathymetry (> 500 m), low concentrations of Chl-a (< 1 μg.L^{-1}), and low dissolved oxygen concentrations (< 100 μmol.kg^{-1}). Low salinity (< 35), latitude (between 13° and 15°N), longitude (east of −17.4°W), combined with bathymetry <500 m and high temperature (> 22 °C) were the main characteristics of D2 and N2 echo-groups. The D3 and N3 echo-groups were mostly explained by high temperature (> 20 °C) and salinity (> 35), while D4 and N4 echo-groups were explained by temperatures ranging from 17°-21 °C, bathymetry <500 m, latitude between 12 and 16°N and longitude west of −17.2°W, combined with high salinity (> 35) and Chl-a concentrations above 1 μg.L^{-1}. The D5 and N5 echo-groups were mostly explained by shallow bathymetry (< 200 m) and low temperature (< 20 °C), latitude north of 14°N and longitude east of −17.4°W. Finally, the N6 echo-group was mostly explained by latitude north of 12.5°N and low salinity (< 35) as well as low temperatures (< 17 °C) but also, to a lesser extent, by higher temperatures (> 21 °C).

3.5. Microscale analysis around a filament

Horizontal and vertical variations in environmental characteristics were observed (Fig. 2 and S26) around the filament located at 13.5°N on 21st December, during a Scanfish transect. Especially, localized concentrations of Chl-a were elevated, coinciding with upwelling waters characterized by lower temperatures, lower dissolved oxygen concentrations and higher salinities. To compare with the echo-group stratifications, the 23 °C isotherm was overlaid over the echogram (Fig. 9). The depth variations of the N2 and N4 echo-groups followed the depth variations of the 23 °C isotherm, with a clear transition between these echo-groups corresponding to the isotherm depth. Hence, effects of the stratification on the N2 and N4 echo-groups were consistent with the horizontal and vertical variations of the environmental variables. No noticeable changes in stratification were observed for the N1 and N6 echo-groups, while the N3 echo-group followed the variations observed for the N4 echo-group.

4. Discussion

By analyzing the acoustic data combined with the environmental variables throughout the water column, we provided new insights into the spatial distribution of organisms in the Senegalese coastal area at the beginning of the upwelling season. We proposed a methodological framework to perform a hierarchical classification of the active acoustic

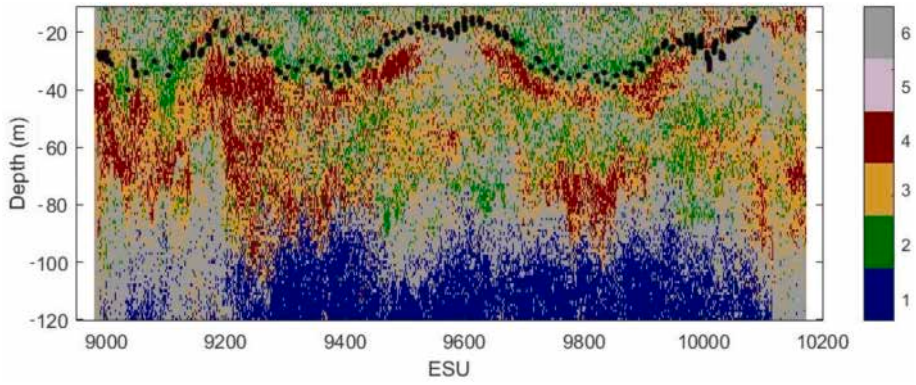

Fig. 9. Echogram showing the echo-groups during nighttime for the filament at 13.5°N. Colors depend on the echo-group (N1: blue, N2: green, N3: orange, N4: red, N5: purple and N6: grey). The black line represents the 23 °C isotherm measured with the Scanfish, which helps visualize environmental variations. ESU means Elementary Sampling Unit. (For interpretation of the references to colour in this figure legend, the reader is referred to the web version of this article.)

data and to relate the defined echo-groups to the environmental variables using a machine learning method (Receveur et al., 2020).

Firstly, the acoustic data were echointegrated before being classified into several echo-groups. To limit computational costs, the integration distance was set to 0.05 nmi (~ 93 m) in the echointegration and the vertical resolution for the echo-integration was set to 1 m. As a result, multiple organisms with different acoustic properties (type, shape and material properties) could be present in the echo-integrated cells. This complicated the interpretation of the frequency response of a given volume backscattering (Benoit-Bird and Lawson, 2016). The integration resolutions could be reduced in the future as greater computing resources become available. Strong gradients in temperature and salinity could also have complicated the interpretation of acoustic scatters, increasing uncertainties about whether the sources of the scattering were biological or physical (Warren et al., 2003). Moreover, for practical reasons, the echosounders were calibrated several months prior to the survey in a different ocean sector (north eastern Atlantic area). Consequently, calibration biases could have occurred due to changes in the water temperature conditions as shown in Demer and Renfree (2008), although the variations were 1 dB or less with temperatures ranging from 1 to 18 °C in their study. However, their tested temperatures were also lower than the ones encountered during our survey.

Nevertheless, our clustering approach revealed several distinct echo-groups having specific frequency responses, with similar echo-groups observed during the day and night. The clustering relied on four frequencies: 38, 70, 120 and 200 kHz. In particular, the 38 kHz has been commonly used to assess the biomass of fish with swimbladders (Receveur et al., 2020; Diogoul et al., 2021) as the swimbladder resonance could induce a high 38-kHz backscatter. However, incorporating a lower frequency, such as 18 kHz, could have improved the discrimination of echo-groups and their biological interpretation. Indeed, the overall shapes of frequency responses differed depending on the types of organisms, as zooplankton resonate more at higher frequencies whereas fish resonate at frequencies lower than 38 kHz (Lavery et al., 2007; Davison et al., 2015). In addition, a frequency lower than 38 kHz could help discriminate fish with large swimbladders, whereas the 38 kHz frequency is more suitable for fish with small swimbladders (Kloser et al., 2002). Finally, the interest of using high frequencies to study zooplankton restricted our classification to the first 120 m depth (the maximum range of the transducer at 200 kHz being 120 m).

One of the major limitations in our study was the low number of trawl samples available, particularly during the daytime, which reduced our ability to validate our echo-group classification. As a result, the correlation matrix using both daytime and nighttime data provided similar results to the one using only nighttime data. This is likely due to the higher organism diversity and biomass observed in night trawls. Increasing the number of trawls could help refine the calculations of the correlation coefficients for each echo-group and strengthen the biological interpretations. Furthermore, our target trawl depths were around 30 m, and avoidance behavior could be more pronounced in both the day and night in the surface layers. Indeed, oganisms could detect the vessel, due to different sources of stimulation such as light or vessel noise (Draštík and Kubečka, 2005). Therefore, a strong avoidance behavior could explain the low catchability rate during daytime, although this behavior is likely to occur also during nighttime. Due to biases in our biological sampling and the limited number of trawl samples, we did not use alternative methods such as the forward scattering approach to predict the acoustic response of trawls, as it requires a thorough knowledge of the taxa present. Especially, Barbin et al. (2024) highlighted significant differences (up to 20 dB) between observed and predicted acoustic responses, particularly in the epipelagic layer, showing that this method is not optimal for these depth ranges. Nevertheless, integrating a forward scattering approach could be valuable to better understand the echo-groups in the mesopelagic layer, where divergence between acoustics and trawls might be smaller.

The methodology used to explain echo-group distribution (as a function of the 3D environment) based on a machine learning approach (XGBoost model) performed better for daytime data than for nighttime. Several explanations could explain these contrasted results. Firstly, the lower predictive power for N2 and N5 could be explained by the low number of samples for these echo-groups. Indeed, the N5 echo-group was mainly found in shallow coastal waters where navigation was limited at night due to intense artisanal fishing activities. Moreover, the nighttime vertical distribution of the organisms associated with the echo-groups could be explained by factors not included in the models such as complex behavioural strategies related to feeding, predation avoidance, community structure or light intensity (Catul et al., 2011). Especially, the DVM is related to feeding strategies (Pearre, 2003), with migrant organisms optimizing their foraging behavior in the productive upper layer. A higher number of mixed organisms in the echo-integration cells at night could also lead to greater uncertainties in hierarchical classification. Nevertheless, the day echo-groups were consistent with the night echo-groups, as seen with the re-calculation the echo-group proportions after excluding the N6 echo-group. This revealed that the proportion of each remaining echo-group was equivalent between daytime and nighttime with D3 and N3 dominating (38–41 %) and D5 and N5 being in minority (3–4 %). Hence, the overall structure of the ecosystem in the epipelagic zone was roughly similar over a daily cycle and from inshore to offshore along the Senegalese coast. The corresponding echo-groups between day and night were impacted by the same environmental variables, highlighting the consistency of the results and the environmental preferences of the underlying organisms.

As in Receveur et al. (2020), bathymetry was one of the most

influential variables in the models for both nighttime and daytime. This result was expected, as we sampled very contrasted areas along the Senegalese coast (inshore vs offshore). Bathymetry also plays a key role in shaping the vertical distribution of the SSLs (thickness and depth) in inshore areas of the Senegalese continental shelf (Diogoul et al., 2020). In addition, bathymetry is suggested to induce school formation in shallow waters, although the relationship remains unclear (Kaltenberg and Benoit-Bird, 2009). In this study, numerous schools were indeed observed in shallow waters, whereas they were scarce in deeper areas. Moreover, water temperature was a key variable for both daytime and nighttime models, while dissolved oxygen concentrations had little influence for the top 120 m of the water column. Latitude constituted a more important variable than longitude for both daytime and nighttime models. Latitude may capture differences in the structuring of the ecosystem along the Senegalese coast (e.g. distinct dynamics in the North and South of the Cape Verde peninsula). Chl-a concentrations were mostly important during daytime, which was not surprising because areas enriched by upwelling dynamics were mainly sampled during the day. Finally, salinity was not a strong explanatory variable of the global models. However, it played a significant role for some echo-groups such as D2 for which low salinities (< 35) had a strong influence and explained its spatial distribution.

Fish schools and large isolated individuals were classified into the D5 and N5 echo-groups, with schools mostly present during daytime. These echo-groups were characterized by high CV values, which served as discriminatory variables. In contrast, SSLs exhibited lower CVs due to their generally homogeneous structure compared to the echo-integrated cells containing schools or isolated fish. Several clustering tests (not shown), excluding the CVs, were inconclusive to classify the D5 and N5 echo-groups, mainly because they were mixed with SSLs having high scatters at 38 kHz. In addition, latitude (14–15°N) and shallow bathymetry (< 200 m) were important variables for explaining their distribution. Indeed, the schools or isolated fish were mostly located in the south of the Cap Vert peninsula based on both night and day data (Fig. 5) which was not surprising as this location represent spawning areas for several SPF species (Boëly et al., 1979; Roy et al., 1989; Ndoye et al., 2017). This area also corresponds to the location of artisanal fisheries during nighttime. Furthermore, the D5 and N5 echo-groups (i.e. pelagic schools) showed preferences for low temperatures (< 20 °C), and their preferential locations were near the coast where the upwelling occured. Sea surface temperature was indeed suggested to be a key environmental variable, combined with Chl-a concentration, upwelling intensity and wind-induced turbulence, for the recruitment success of *S. aurita* and *S. maderensis* (Diankha et al., 2018). Diankha et al. (2015) also found that high abundances of round sardinella in Senegalese waters were associated with temperature ranging from 21 to 25 °C. These temperatures were higher than the ones found for D5 and N5, but this shift could be explained by the fact that their data were computed from satellite SST. Indeed, fish schools were often observed close to the bottom where water temperatures were systematically 4–6 °C lower than at the surface. Other factors such as food availability could explain fish spatial distributions but were not included in the model. Finally, the D5 and N5 echo-groups were also positively correlated to other fish families, such as Sphyraenidae, Scombridae. and Priacanthidae, which could be responsible for strong echoes. Tunas were also spotted during the survey. Accordingly, we associated the D5 and N5 echogroups to large fish and fish schools with a high degree of confidence.

The D4 and N4 echo-groups were attributed to small fish or fish larvae as their frequency curves decreased between 38 and 200 kHz (Kloser et al., 2002; Lavery et al., 2007). These echo-groups were aggregated into layers having strong scatters at 38 kHz. In addition, the thermal preferences of D4 and N4 were found to be between 17° and 21 °C and the associated SSLs were located below the thermocline. Correlations between the depth of the thermocline and the depth of SSLs was shown in previous studies (Marchal et al., 1993; Diogoul et al., 2020). Nevertheless, further analysis would be required to better understand the links between stratification of the SSLs and temperature, as this variable could be a proxy for hydrographic features reflecting different oceanographic conditions. Diogoul et al. (2020) also attributed the SSLs which scatters more strongly at 38 kHz than at higher frequencies to small fish or fish larvae. The authors suggested that these small fish or fish larvae could originate from nursery areas as juveniles of numerous species concentrate there. The D3 and N3 echo-groups exhibited frequency response curves similar to those of the D4 and N4 echo-groups, also suggesting their association with small fish or fish larvae. However, D3 and N3 differed by a lower scattering intensity at 38 kHz (Fig. 4c,h). A hypothesis compatible with this result is that the D3 and N3 echo-groups were composed of more mixed types of organisms, explaining a global lower scattering at 38 kHz. Indeed, these echo-groups were positively correlated to other types of organisms (gelatinous and crustaceans). This hypothesis could be supported by the higher CVs values for D3 and N3 than for D4 and N4. The distinctions between these echo-groups (D3 vs D4, N3 vs N4) could also be explained by a difference in terms of biomass for fish larvae and small fish. The results would then suggest that small fish and larvae are distributed along the Senegalese coast where D3, D4, N3 and N4 echo-groups are identified, with patches of higher abundance corresponding to D4 and N4. Ndour et al. (2018) found low densities of eggs and fish larvae along the Senegal-Guinea coast, but high densities of fish eggs were reported in the south of Dakar and high density of larvae off Casamance. Their study also identified Clupeidae as the dominant larval family (35.8 %), followed by Myctophidae (14.3 %). Coupling our results with additional samplings of organisms would be necessary to go further in the analyses.

Six echo-groups were identified during nighttime versus five during daytime. We associated the N6 echo-group with the organisms performing DVM. This hypothesis was supported by trawl analyses and visual inspections of the echogram showing DVM patterns for this layer. We suggested that this N6 echo-group was a mixed echo-group composed of MTLOs performing DVM, as indicated by the correlation matrices (Fig. 6b,c), but that their frequency response was mainly driven by micronektonic fish having stronger scattering. The proportion of migrant organisms was preponderant during nighttime (39 %). The N6 echo-group can be associated with diurnal migratory organisms with high confidence. This echo-group was predominant and ubiquitous along the Senegalese coast (Fig. 5), suggesting its crucial ecological role for the ecosystem (Catul et al., 2011). Indeed, myctophids could represent a significant energy source for marine predators (Lea et al., 2002; Goetsch et al., 2018). The migration depth of the N6 echo-group during nighttime was mainly located below the surface boundary layer, with denser layers around 20–50 m-depth. This is consistent with previous studies reporting that the preferred nighttime depth location of myctophids is around the thermocline, where prey concentrations are greater (Rissik and Suthers, 2000; Peña et al., 2014).

The D2 and N2 echo-groups exhibited frequency responses that were characteristic of gas-bearing organisms, such physonects or cystonects siphonophores (Warren et al., 2001; Lavery et al., 2007; Blanluet et al., 2019), for which the pneumatophore is responsible for the strong acoustic return. Nevertheless, the presence of siphonophores in trawls was low, which could explain the low correlations with the N2 echo-group (Fig. 6b). This discrepancy could be attributed to the fragility of these organisms, which are likely to be damaged or destroyed during trawling (Lavery et al., 2007; Davison et al., 2015). Some locations in the south of Dakar presented higher D2 and N2 acoustic density and were similar to the ones of the D3, D4 and N3 and N4 echo-group as seen on Fig. 5. Uribe-Palomino et al. (2019) found positive correlations between siphonophore abundances and those of copepods and fish eggs. Indeed, siphonophores are known to feed on copepods and fish larvae (Purcell, 1985). Hence, this could explain their co-location with the D4 and N4 echo-groups, corresponding to fish larvae and small fish, especially during nighttime. In addition, temperature, salinities and dissolved oxygen were found to affect siphonophores communities with positive or negative correlations depending on the species (Zoeller et al., 2022).

Here, both D2 and N2 were better explained by high temperatures (> 22 °C), low salinities (< 35) and to a lesser extent high dissolved oxygen concentrations (> 150 μmol.kg^{-1}) irrespective of the time of the day, suggesting that the same communities were observed during daytime and nighttime.

Finally, the D1 and N1 echo-groups showed increasing frequency response curves from 70 to 333 kHz which could suggest fluid-like zooplankton (Lavery et al., 2007). These echo-groups were in fact positively correlated to shrimps, euphausiids and other crustaceans, the trawl mesh was however not suitable for sampling copepods. Overall, the wide diversity of zooplankton species with distinct anatomical features could result in high variability in the scattering properties (Stanton et al., 1994a). In addition, the presence of a peak at 38 kHz on the frequency response curves of D1 and N1 suggested that other types of organisms could have been present in the echo-integrated cells. A similar shape curve can be observed in Barbin et al. (2024), resulted from a mix of pteropods and fish with swimbladders. Indeed, a limitation of our acoustic study is that zooplankton scatters may be polluted by stronger scatters (Lavery et al., 2007) such as fish schools and SSLs, inducing a classification bias. In addition, the D1 and N1 echo-groups were observed at all depth and bathymetries but were mainly found offshore and at depth deeper than 60 m, where the other echo-groups were absent. These locations were characterized by low temperature (< 18 °C) and low dissolved oxygen concentrations (< 100 μmol.kg^{-1}), explaining why these variables were important in the models. Consequently, these results should be taken with caution as they may result from classification bias. Especially, specific zooplankton samplings during the survey showed that fluid-like zooplankton were found at all depths (data not shown). In addition, zooplankton samplings taken along the Senegal-Guinea coast showed that copepods are dominant (68.5 %) (Ndour et al., 2018), with important biomass near the coast. The difference with our results may also have arisen due to temporal variability in the upwelling activity and how it impacts species abundance. Indeed, high zooplankton abundance was found offshore during the warm season by Diouf (1991). Therefore, interpreting zooplankton distribution is complex as their classification was not straightforward. To go further, reducing the echo-integration resolution could help to better classify these organisms by limiting the mixing of organisms.

Although more acoustic data in the upwelling context would be needed to draw robust general conclusions, our study showed that the vertical distribution of N2 and N4 echo-groups followed the variations of the 23 °C isotherm depth (Fig. 9). This isotherm was a proxy of the thermocline location and its position changes reflected those of the oceanographic conditions. Specifically, the upwelling of cold and deep nutrient-rich waters enhanced the presence of the N4 echo-groups in the upper water column. The role of upwelling intensity on pelagic fish abundances, such as *S. aurita*, has been previously established (Braham et al., 2014; Mbaye et al., 2015; Diankha et al., 2018). Larvae of fish species that reproduce near the coast have been observed within upwelling filament structures near the Canary Islands (Rodríguez et al. JM et al., 1999, Bécognée et al., 2009), with the filament acting as a mechanism transporting the larvae away from the African continent. As the N4 echo-group is thought to be representative of small fish or fish larvae, our results are consistent with studies suggesting that filaments influence fish larvae spatial distributions, inducing changes in their vertical distributions. Nevertheless, applying our methodology to other filament observations would allow to draw more robust conclusions.

5. Conclusions

Our study revealed different spatial distributions of several echo-groups along the Senegalese coast during the upwelling period, identified through a hierarchical classification of the acoustic data. The echo-groups exhibited distinct scattering characteristics, allowing us to hypothesize the type of organisms responsible of the echoes. Fish schools were mostly located in shallow coastal waters, whereas migrant organisms were ubiquitous in the ecosystem and predominant during nighttime. In addition, the environmental data measured in the water column allowed us to better identify the environmental preferences of the organisms. By using two machine learning models, we found that these preferences were similar during nighttime and daytime. Our methodology provided new insights into the spatial distributions of the different organisms in the NW African upwelling ecosystem, which is crucial for improving ecosystem-based management.

CRediT authorship contribution statement

Viviane David: Writing – review & editing, Writing – original draft, Methodology, Investigation, Formal analysis, Conceptualization. **Jérémie Habasque:** Writing – review & editing, Supervision, Methodology, Investigation, Conceptualization. **Gildas Roudaut:** Supervision, Methodology, Investigation, Conceptualization. **Louis Marie:** Methodology, Investigation, Formal analysis, Conceptualization. **Delphine Thibault:** Writing – review & editing, Investigation, Formal analysis, Conceptualization. **Anne Lebourges-Dhaussy:** Writing – review & editing, Supervision, Project administration, Methodology, Conceptualization. **Xavier Capet:** Writing – review & editing, Supervision, Resources, Project administration, Methodology, Investigation, Funding acquisition, Conceptualization. **Eric Machu:** Writing – review & editing, Supervision, Resources, Project administration, Methodology, Investigation, Funding acquisition, Conceptualization.

Declaration of competing interest

The authors declare that they have no known competing financial interests or personal relationships that could have appeared to influence the work reported in this paper.

Acknowledgement

The authors would like to thank the RV Thalassa Captain Loïc Provost, his crew and all the scientists involved in the SCOPES surveys. In particular, we would like to thank Olivier Peden, Sébastien Prigent and Olivier Ménage in particular for their useful help with the Scanfish. This work was supported by the French oceanographic fleet ("Flotte Océanographique Française") as well as the French Agence nationale de la recherche (grant SOLAB ANR-18- CE32- 0009). The authors also wish to thank the two anonymous reviewers for their helpful comments and suggestions of improvement.

Appendix A. Supplementary data

Supplementary data to this article can be found online at https://doi.org/10.1016/j.jmarsys.2025.104113.

Data availability

Data will be made available on request.

References

Ariza, A., Garijo, J.C., Landeira, J.M., Bordes, F., Hernández-León, S., 2015. Migrant biomass and respiratory carbon flux by zooplankton and micronekton in the subtropical Northeast Atlantic Ocean (Canary Islands). Prog. Oceanogr. 134, 330–342.

Auger, P.-A., Gorgues, T., Machu, E., Aumont, O., Brehmer, P., 2016. What drives the spatial variability of primary productivity and matter fluxes in the north-west African upwelling system? A modelling approach. Biogeosciences 13, 6419–6440.

Ba, K., Thiaw, M., Lazar, N., Sarr, A., Brochier, T., Ndiaye, I., Faye, A., Sadio, O., Panfili, J., Thiaw, O.T., Brehmer, P., 2016. Resilience of key biological parameters of the Senegalese flat Sardinella to overfishing and climate change. PLoS One 11, e0156143.

Ballón, M., Bertrand, A., Lebourges-Dhaussy, A., Gutiérrez, M., Ayón, P., Grados, D., Gerlotto, F., 2011. Is there enough zooplankton to feed forage fish populations off Peru? An acoustic (positive) answer. Prog. Oceanogr. 91, 360.

Barbin, L., Lebourges-Dhaussy, A., Allain, V., Receveur, A., Lehodey, P., Habasque, J., Vourey, E., Portal, A., Roudaut, G., Menkes, C., 2024. Comparative analysis of day and night micronekton abundance estimates in West Pacific between acoustic and trawl surveys. Deep Sea Res. Part Oceanogr. Res. Pap. 204, 104221.
Bécognée, P., Moyano, M., Almeida, C., Rodríguez, J.M., Fraile-Nuez, E., Hernández-Guerra, A., Hernández-León, S., 2009. Mesoscale distribution of clupeoid larvae in an upwelling filament trapped by a quasi-permanent cyclonic eddy off Northwest Africa. Deep Sea Res. Part Oceanogr. Res. Pap. 56, 330–343.
Béhagle, N., Cotté, C., Lebourges-Dhaussy, A., Roudaut, G., Duhamel, G., Brehmer, P., Josse, E., Cherel, Y., 2017. Acoustic distribution of discriminated micronektonic organisms from a bi-frequency processing: the case study of eastern Kerguelen oceanic waters. Prog. Oceanogr. 156, 276–289.
Belhabib, D., Koutob, V., Sall, A., Lam, V.W.Y., Pauly, D., 2014. Fisheries catch misreporting and its implications: the case of Senegal. Fish. Res. 151, 1–11.
Benoit-Bird, K.J., Lawson, G.L., 2016. Ecological insights from pelagic habitats acquired using active acoustic techniques. Annu. Rev. Mar. Sci. 8, 463–490.
Bertrand, A., Bard, F.-X., Josse, E., 2002. Tuna food habits related to the micronekton distribution in French Polynesia. Mar. Biol. 140, 1023–1037.
Bianchi, D., Galbraith, E.D., Carozza, D.A., Mislan, K.S., Stock, C.A., 2013. Intensification of open-ocean oxygen depletion by vertically migrating animals. Nat. Geosci. 6, 545–548.
Blanluet, A., Doray, M., Berger, L., Romagnan, J.-B., Bouffant, N.L., Lehuta, S., Petitgas, P., 2019. Characterization of sound scattering layers in the Bay of Biscay using broadband acoustics, nets and video. PLoS One 14, e0223618.
Boëly, T., Chabanne, J., Fréon, P., 1979. Schémas migratoires, aires de concentrations et périodes de reproduction des principales espèces de poissons pélagiques côtiers dans la zone sénégalo-mauritanienne. Comm Pêch Pour Atl Cent-EstProceedings Dakar.
Bollens, S.M., Frost, B.W., 1989a. Predator-induced diet vertical migration in a planktonic copepod. J. Plankton Res. 11, 1047–1065.
Bollens, S.M., Frost, B.W., 1989b. Zooplanktivorous fish and variable diel vertical migration in the marine planktonic copepod *Calanus pacificus*. Limnol. Oceanogr. 34, 1072–1083.
Braham, C.-B., Fréon, P., Laurec, A., Demarcq, H., Bez, N., 2014. New insights in the spatial dynamics of sardinella stocks off Mauritania (North-West Africa) based on logbook data analysis. Fish. Res. 154, 195–204.
Brodeur, R., Seki, M., Pakhomov, E., Suntsov, A., 2005. Micronekton-What are they and Why are they Important ?.
Brown, J., Brander, K., Fernand, L., Hill, A., 1997. Scanfish: high performance towed undulator. Oceanogr. Lit. Rev. 44.
Capet, X., Estrade, P., Machu, E., Ndoye, S., Grelet, J., Lazar, A., Marié, L., Dausse, D., Brehmer, P., 2017. On the dynamics of the southern Senegal upwelling center: observed variability from synoptic to Superinertial scales. J. Phys. Oceanogr. 47, 155–180.
Carr, M.-E., Kearns, E.J., 2003. Production regimes in four eastern boundary current systems. Deep Sea Res. Part II Top Stud. Oceanogr. 50, 3199–3221.
Catul, V., Gauns, M., Karuppasamy, P.K., 2011. A Review on Mesopelagic Fishes Belonging to Family Myctophidae.
Chen, T., Guestrin, C., 2016. XGBoost: a scalable tree boosting system. In: Proceedings of the 22nd ACM SIGKDD International Conference on Knowledge Discovery and Data Mining. KDD '16. Association for Computing Machinery, New York, NY, USA, pp. 785–794.
Choi, C., Kampffmeyer, M., Handegard, N.O., Salberg, A.-B., Brautaset, O., Eikvil, L., Jenssen, R., 2021. Semi-supervised target classification in multi-frequency echosounder data. ICES J. Mar. Sci. 78, 2615–2627.
Cotté, C., Ariza, A., Berne, A., Habasque, J., Lebourges-Dhaussy, A., Roudaut, G., Espinasse, B., Hunt, B.P.V., Pakhomov, E.A., Henschke, N., Péron, C., Conchon, A., Koedooder, C., Izard, L., Cherel, Y., 2022. Macrozooplankton and micronekton diversity and associated carbon vertical patterns and fluxes under distinct productive conditions around the Kerguelen Islands. J. Mar. Syst. 226, 103650.
Cury, P., Roy, C., 1989. Optimal environmental window and pelagic fish recruitment success in upwelling areas. Can. J. Fish. Aquat. Sci. 46, 670–680.
Cushing, D.H., 1951. The vertical migration of planktonic Crustacea. Biol. Rev. 26, 158–192.
David, V., Mouget, A., Thiriet, P., Minart, C., Perrot, Y., Le Goff, L., Bianchimani, O., Basthard-Bogain, S., Estaque, T., Richaume, J., Sys, J.-F., Cheminée, A., Feunteun, E., Acou, A., Brehmer, P., 2024. Species identification of fish shoals using coupled split-beam and multibeam echosounders and two scuba-diving observational methods. J. Mar. Syst. 241, 103905.
Davison, P.C., Koslow, J.A., Kloser, R.J., 2015. Acoustic biomass estimation of mesopelagic fish: backscattering from individuals, populations, and communities. ICES J. Mar. Sci. 72, 1413–1424.
De Robertis, A., Higginbottom, I., 2007. A post-processing technique to estimate the signal-to-noise ratio and remove echosounder background noise. ICES J. Mar. Sci. 64, 1282–1291.
De Robertis, A., McKelvey, D.R., Ressler, P.H., 2010. Development and application of an empirical multifrequency method for backscatter classification. Can. J. Fish. Aquat. Sci. 67, 1459–1474.
Demarcq, H., Faure, V., 2000. Coastal upwelling and associated retention indices derived from satellite SST. Application to *Octopus vulgaris* recruitment. Oceanol. Acta 23, 391–408.
Demarcq, H., Samb, B., 1991. Influence des variations de l'upwelling sur la répartition des poissons pélagiques au Sénégal. In: Pêcheries ouest africaines : variabilité, instabilité et changement, Cury Philippe, Roy Claude. Groupes de Travail, Dakar; Casablanca (SEN; MAR), 1988/12/12-17, pp. 290–306.
Demer, D.A., Renfree, J.S., 2008. Variations in echosounder–transducer performance with water temperature. ICES J. Mar. Sci. 65, 1021–1035.
Demer, D.A., Berger, L., Bernasconi, M., Bethke, E., Boswell, K., Chu, D., Domokos, R., Dunford, A., Fassler, S., Gauthier, S., Hufnagle, L.T., Jech, J.M., Bouffant, N., Lebourges-Dhaussy, A., Lurton, X., Macaulay, G.J., Perrot, Y., Ryan, T., Parker-Stetter, S., Stienessen, S., Weber, T., Williamson, N., 2015. Calibration of Acoustic Instruments. International Council for the Exploration of the Sea (ICES).
Diankha, O., Thiaw, M., Sow, B.A., Brochier, T., Gaye, A.T., Brehmer, P., 2015. Round sardinella (*Sardinella aurita*) and anchovy (*Engraulis encrasicolus*) abundance as related to temperature in the senegalese waters. Thalassas 31, 9–17.
Diankha, O., Ba, A., Brehmer, P., Brochier, T., Sow, B.A., Thiaw, M., Gaye, A.T., Ngom, F., Demarcq, H., 2018. Contrasted optimal environmental windows for both sardinella species in Senegalese waters. Fish. Oceanogr. 27, 351–365.
Diogoul, N., Brehmer, P., Perrot, Y., Tiedemann, M., Thiam, A., El Ayoubi, S., Mouget, A., Migayrou, C., Sadio, O., Sarré, A., 2020. Fine-scale vertical structure of sound-scattering layers over an east border upwelling system and its relationship to pelagic habitat characteristics. Ocean Sci. 16, 65–81.
Diogoul, N., Brehmer, P., Demarcq, H., El Ayoubi, S., Thiam, A., Sarre, A., Mouget, A., Perrot, Y., 2021. On the robustness of an eastern boundary upwelling ecosystem exposed to multiple stressors. Sci. Rep. 11, 1908.
Diogoul, N., Brehmer, P., Kiko, R., Perrot, Y., Lebourges-Dhaussy, A., Rodrigues, E., Thiam, A., Mouget, A., Ayoubi, S.E., Sarré, A., 2024. Estimating the copepod biomass in the north west African upwelling system using a bi-frequency acoustic approach. PLoS One 19, e0308083.
Diouf, P. Samba, 1991. Le zooplancton au Sénégal. In: Philippe, Cury, Claude, Roy (Eds.), Pêcheries ouest africaines : variabilité, instabilité et changement. Groupes de Travail, Dakar; Casablanca (SEN; MAR), 1988/12/12–17.
Draštík, V., Kubečka, J., 2005. Fish avoidance of acoustic survey boat in shallow waters. Fish. Res. 72, 219–228.
FAO, 2013. Working Group on the Assessment of the Small Pelagic Fish off Northwest Africa.
Foote, K.G., 1987. Fish target strengths for use in echo integrator surveys. J. Acoust. Soc. Am. 82, 981–987.
Fréon, P., 1983. Production models as applied to sub-stocks depending on upwelling fluctuations. In: Proceedings of the Expert Consultation to Examine Changes in Abundance and Species Composition of Neritic Fish Resources. Expert Consultation to Examine Changes in Abundance and Species Composition of Neritic Fish Resources. FAO, Rome, pp. 1047–1064.
Goetsch, C., Conners, M.G., Budge, S.M., Mitani, Y., Walker, W.A., Bromaghin, J.F., Simmons, S.E., Reichmuth, C., Costa, D.P., 2018. Energy-rich mesopelagic fishes revealed as a critical prey resource for a deep-diving predator using quantitative fatty acid signature analysis. Front. Mar. Sci. 5.
Hays, G.C., 2003. A review of the adaptive significance and ecosystem consequences of zooplankton diel vertical migrations. Hydrobiologia 503, 163–170.
Hays, G., Harris, R., Head, R., 1997. The vertical nitrogen flux caused by zooplankton diel vertical migration. Mar. Ecol. Prog. Ser. 160, 57–62.
James, A.G., 1988. Are clupeid microphagists herbivorous or omnivorous? A review of the diets of some commercially important clupeids. South Afr. J. Mar. Sci. 7, 161–177.
JM, Rodríguez, Hernández-León, S., Barton, E.D., 1999. Mesoscale distribution of fish larvae in relation to an upwelling filament off Northwest Africa. Deep Sea Res. Part Oceanogr. Res. Pap. 46, 1969–1984.
Kaltenberg, A., Benoit-Bird, K., 2009. Diel Behavior of Sardine and Anchovy Schools in the California Current System.
Klevjer, T.A., Irigoien, X., Røstad, A., Fraile-Nuez, E., Benítez-Barrios, V.M., Kaartvedt, S., 2016. Large scale patterns in vertical distribution and behaviour of mesopelagic scattering layers. Sci. Rep. 6, 19873.
Kloser, R.J., Ryan, T., Sakov, P., Williams, A., Koslow, J.A., 2002. Species identification in deep water using multiple acoustic frequencies. Can. J. Fish. Aquat. Sci. 59, 1065–1077.
Kounta, L., Capet, X., Jouanno, J., Kolodziejczyk, N., Sow, B., Gaye, A.T., 2018. A model perspective on the dynamics of the shadow zone of the eastern tropical North Atlantic – Part 1: the poleward slope currents along West Africa. Ocean Sci. 14, 971–997.
Kuhn, M., 2008. Building predictive models in R using the caret package. J. Stat. Softw. 28, 1–26.
Lampert, W., 1989. The adaptive significance of diel vertical migration of zooplankton. Funct. Ecol. 3, 21–27.
Lathuilière, C., Echevin, V., Lévy, M., 2008. Seasonal and intraseasonal surface chlorophyll-a variability along the northwest African coast. J. Geophys. Res. Oceans 113.
Lavery, A.C., Wiebe, P.H., Stanton, T.K., Lawson, G.L., Benfield, M.C., Copley, N., 2007. Determining dominant scatterers of sound in mixed zooplankton populations. J. Acoust. Soc. Am. 122, 3304–3326.
Lavery, A.C., Chu, D., Moum, J.N., 2010. Measurements of acoustic scattering from zooplankton and oceanic microstructure using a broadband echosounder. ICES J. Mar. Sci. 67, 379–394.
Lea, M.-A., Nichols, P.D., Wilson, G., 2002. Fatty acid composition of lipid-rich myctophids and mackerel icefish (*Champsocephalus gunnari*) – Southern Ocean food-web implications. Polar Biol. 25, 843–854.
Lehodey, P., Conchon, A., Senina, I., Domokos, R., Calmettes, B., Jouanno, J., Hernandez, O., Kloser, R., 2015. Optimization of a micronekton model with acoustic data. ICES J. Mar. Sci. 72, 1399–1412.
Lett, C., Roy, C., Levasseur, A., Van Der Lingen, C.D., Mullon, C., 2006. Simulation and quantification of enrichment and retention processes in the southern Benguela upwelling ecosystem. Fish. Oceanogr. 15, 363–372.
Lundberg, S.M., Lee, S.-I., 2017. A unified approach to interpreting model predictions | BibSonomy. In: Guyon, I., Luxburg, U.V., Bengio, S., Wallach, H., Fergus, R.,

Vishwanathan, S., Garnett, R., Maclennan, D.N., Fernandes, P.G. (Eds.), Advances in Neural Information Processing Systems, 30. Dalen, Curran Associates, Inc., pp. 4765–4774
MacLennan, D.N., Fernandes, P.G., Dalen, J., 2002. A consistent approach to definitions and symbols in fisheries acoustics. ICES J. Mar. Sci. 59, 365–369.
Marchal, E., Gerlotto, F., Stequert, B., 1993. On the relationship between scattering layer, thermal structure and tuna abundance in the eastern Atlantic equatorial current system. Oceanol. Acta 16, 261–272.
Mbaye, B.C., Brochier, T., Echevin, V., Lazar, A., Lévy, M., Mason, E., Gaye, A.T., Machu, E., 2015. Do *Sardinella aurita* spawning seasons match local retention patterns in the Senegalese–Mauritanian upwelling region? Fish. Oceanogr. 24, 69–89.
Messié, M., Chavez, F.P., 2015. Seasonal regulation of primary production in eastern boundary upwelling systems. Prog. Oceanogr. Complete 1–18.
Mouget, A., Brehmer, P., Perrot, Y., Uanivi, U., Diogoul, N., El Ayoubi, S., Jeyid, M.A., Sarré, A., Béhagle, N., Kouassi, A.M., Feunteun, E., 2022. Applying acoustic scattering layer descriptors to depict mid-trophic pelagic organisation: the case of Atlantic African large marine ecosystems continental shelf. Fishes 7, 86.
Mutlu, E., 2006. Diel vertical migration of *Sagitta setosa* as inferred acoustically in the Black Sea. Mar. Biol. 149, 573–584.
Mutlu, E., 2007. Compared studies on recognition of marine underwater biological scattering layers. J. Appl. Biol. Sci. 1, 113–119.
Ndour, I., Berraho, A., Fall, M., Omar, E., Birane, S., 2018. Composition, distribution and abundance of zooplankton along the Senegal-Guinea maritime zone (West Africa). Egypt. J. Aquat. Res. 44, 109–124.
Ndoye, S., Capet, X., Estrade, P., Sow, B., Dagorne, D., Lazar, A., Gaye, A., Brehmer, P., 2014. SST patterns and dynamics of the southern Senegal-Gambia upwelling center. J. Geophys. Res. Oceans 119, 8315–8335.
Ndoye, S., Capet, X., Estrade, P., Sow, B., Machu, E., Brochier, T., Döring, J., Brehmer, P., 2017. Dynamics of a "low-enrichment high-retention" upwelling center over the southern Senegal shelf. Geophys. Res. Lett. 44, 5034–5043.
Pearre, S., 2003. Eat and run? The hunger/satiation hypothesis in vertical migration: history, evidence and consequences. Biol. Rev. Camb. Philos. Soc. 78, 1–79.
Peña, M., Olivar, M.P., Balbín, R., López-Jurado, J.L., Iglesias, M., Miquel, J., 2014. Acoustic detection of mesopelagic fishes in scattering layers of the Balearic Sea (western Mediterranean). Can. J. Fish. Aquat. Sci. 71, 1186–1197.
Perrot, Y., Brehmer, P., Habasque, J., Roudaut, G., Behagle, N., Sarre, A., Lebourges Dhaussy, A., 2018. Matecho : an open-source tool for processing fisheries acoustics data. Acoust Aust. 46, 241–248.
Petersen, W., 2014. FerryBox systems: state-of-the-art in Europe and future development. J. Mar. Syst. 140, 4–12.
Purcell, J.E., 1985. Predation on fish eggs and larvae by pelagic cnidarians and ctenophores. Bull. Mar. Sci. 37, 739–755.
Receveur, A., Menkes, C., Allain, V., Lebourges-Dhaussy, A., Nerini, D., Mangeas, M., Ménard, F., 2020. Seasonal and spatial variability in the vertical distribution of pelagic forage fauna in the Southwest Pacific. Deep Sea Res. Part II Top Stud. Oceanogr. 175, 104655.
Rissik, D., Suthers, I., 2000. Enhanced feeding by pelagic juvenile myctophid fishes within a region of island-induced flow disturbance in the Coral Sea. Mar. Ecol. Prog. Ser. 203, 263–273.
Ross, T., Gaboury, I., Lueck, R., 2007. Simultaneous acoustic observations of turbulence and zooplankton in the ocean. Deep Sea Res. Part Oceanogr. Res. Pap. 54, 143–153.
Roy, C., 1998. An upwelling-induced retention area off Senegal : a mechanism to link upwelling and retention processes. South Afr. J. Mar. Sci. 19, 89–98.
Roy, C., Cury, P., Fontana, A., Belvèze, H., 1989. Stratégies spatio-temporelles de la reproduction des clupéidés des zones d'upwelling d'Afrique de l'Ouest. Aquat. Living Resour. 2, 21–29.
Sarré, A., 2017. Approche acoustique de la dynamique et la distribution spatiale des ressources halieutiques de petits pélagiques dans l'upwelling sénégalo-mauritanien. phdthesis, Université de Bretagne occidentale - Brest.
Stanton, T.K., Chu, D., 2000. Review and recommendations for the modelling of acoustic scattering by fluid-like elongated zooplankton: euphausiids and copepods. ICES J. Mar. Sci. 57, 793–807.
Stanton, T.K., Wiebe, P.H., Chu, D., Benfield, M.C., Scanlon, L., Martin, L., Eastwood, R. L., 1994a. On acoustic estimates of zooplankton biomass. ICES J. Mar. Sci. 51, 505–512.
Stanton, T.K., Wiebe, P.H., Chu, D., Goodman, L., 1994b. Acoustic characterization and discrimination of marine zooplankton and turbulence. ICES J. Mar. Sci. 51, 469–479.
Stanton, T.K., Chu, D., Wiebe, P.H., 1998. Sound scattering by several zooplankton groups. II. Scattering models. J. Acoust. Soc. Am. 103, 236–253.
Strub, P.T., Kosro, P.M., Huyer, A., 1991. The nature of the cold filaments in the California current system. J. Geophys. Res. Oceans 96, 14743–14768.
Štrumbelj, E., Kononenko, I., 2014. Explaining prediction models and individual predictions with feature contributions. Knowl. Inf. Syst. 3, 647–665.
Uribe-Palomino, J., López, R., Gibbons, M.J., Gusmão, F., Richardson, A.J., 2019. Siphonophores from surface waters of the Colombian Pacific Ocean. J. Mar. Biol. Assoc. U. K. 99, 67–80.
Warren, J.D., Stanton, T.K., Benfield, M.C., Wiebe, P.H., Chu, D., Sutor, M., 2001. In situ measurements of acoustic target strengths of gas-bearing siphonophores. ICES J. Mar. Sci. 58, 740–749.
Warren, J.D., Stanton, T.K., Wiebe, P.H., Seim, H.E., 2003. Inference of biological and physical parameters in an internal wave using multiple-frequency, acoustic-scattering data. ICES J. Mar. Sci. 60, 1033–1046.
Zedel, L., Patro, R., Knutsen, T., 2005. Fish behaviour and orientation-dependent backscatter in acoustic Doppler profiler data. ICES J. Mar. Sci. 62, 1191–1201.
Zoeller, V., Canepa, A., Palma, S., 2022. Siphonophore community biodiversity and spatio-temporal distribution concerning the oceanographic parameters in the Patagonian Fjord ecosystem during the winter season. Lat. Am. J. Aquat. Res. 50, 364–381.